Chemical Engineering Journal 318 (2017) 89–94

Contents lists available at ScienceDirect

Chemical Engineering Journal

journal homepage: www.elsevier.com/locate/cej

Modified ilmenite as catalyst for CWPO-Photoassisted process under LED light

P. García-Muñoz [a,*], G. Pliego [a], J.A. Zazo [a], B. Barbero [b], A. Bahamonde [c], J.A. Casas [a]

[a] Sección departamental de Ingeniería Química, Facultad de Ciencias, Universidad Autónoma de Madrid, 28049 Madrid, Spain
[b] Instituto de Investigaciones en Tecnología Química (INTEQUI), UNSL–CONICET, Chacabuco 917, D5700BWS San Luis, Argentina
[c] Instituto de Catálisis y Petroleoquímica (CSIC), C/Marie Curie, 2, 28049 Madrid, Spain

HIGHLIGHTS

- Raw ilmenite was treated to evaluate the influence of iron oxidation state.
- The co-presence of different iron oxidation states led to a faster mineralization.
- Phenol total conversion and 95% of TOC removal was reached in all cases.
- Long-term experiments confirmed the stability of these materials.

GRAPHICAL ABSTRACT

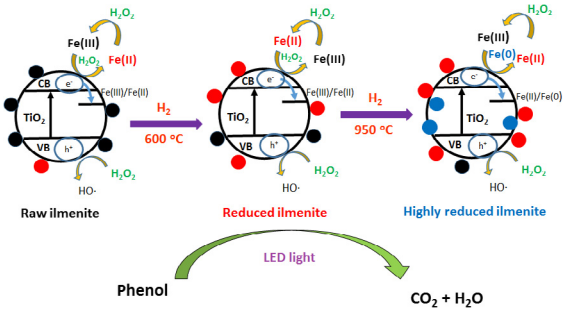

ARTICLE INFO

Article history:
Available online 21 May 2016

Keywords:
Ilmenite
CWPO
Photoassisted
LED
Intensification

ABSTRACT

The influence of the iron chemical nature contained in ilmenite ($FeTiO_3$) upon the activity and stability of these materials as catalysts for CWPO-Photoassisted process under LED light (λ: 405 nm) were evaluated. Raw ilmenite was treated with H_2 within the range 25–1000 °C in order to partially reduce iron oxides to Fe(0). The catalysts were characterized by N_2 adsorption/desorption, TXRF, XRD and XPS analysis. The co-presence of different iron species (Fe(0), Fe(II) and Fe(III)) along with the light effect over material surface, led to an increase of H_2O_2 decomposition rate into HO· and, therefore, a higher oxidation rate. In all case, after total H_2O_2 depletion, a complete phenol degradation and a 95% TOC conversion was reached in batch at $pH_0 = 3$ and 50 °C using the stoichiometric H_2O_2 dose (14 mol H_2O_2/mol phenol) and 10 W m^{-2} LED light. Long-term continuous experiments were carried out to assess the stability and the lifetime of the catalyst. The higher reduction degree led to a higher organic matter mineralization but also to a higher leaching of active phase around 3% of the total iron amount in ilmenite. Nevertheless, catalyst deactivation seems to be related to the oxidation of iron on the catalyst surface.

1. Introduction

Nowadays, water pollution concerns a major issue of increasing importance. The water scarcity beside to the increasingly presence of refractory pollutants force the policymakers to enact stringent wastewater regulation to control the discharge of toxic and non-biodegradable organic compounds in waterbodies.

The EU Water Framework Directive [1] establishes a list of priority pollutants that must receive a special attention to be removed from water because their variety, toxicity and persistence impact the health of ecosystems. Among them, phenols are well known for their bio-recalcitrant and toxicity. They are continuously introduced into the aquatic environment as a result of several industries activities such as the manufacture of pesticides, biocides, resins,

* Corresponding author at: Ingeniería Química, Facultad de Ciencias, C/Francisco Tomás y Valiente 7, Universidad Autónoma de Madrid, 28049 Madrid, Spain.
E-mail address: patricia.garciam@uam.es (P. García-Muñoz).

http://dx.doi.org/10.1016/j.cej.2016.05.093
1385-8947/

dyes, pharmaceuticals. Due to their importance, it has become a challenge to achieve the effective removal of persistent organic pollutants from wastewaters to minimize the risk of pollution problems [2–6].

Advanced Oxidation Processes (AOPs) have been successfully applied for the removal or degradation of a wide variety of recalcitrant pollutants in water. AOPs involves the generation of $HO^{\cdot}_{x}$ radicals that are able to oxidise the organic chemical compounds up to CO_2 and H_2O. Among these processes, Catalytic Wet Peroxide Oxidation (CWPO) and photocatalysis have demonstrated their effectively to remove pollutants. Because of its iron and titanium content, ilmenite results a promising solid for CWPO and photocatalysis treatments [3,7–10]. Nevertheless, it shows significant drawbacks related to a high induction period (in CWPO) and lower activity, due to a high electron-hole recombination (in photocatalysis). A previous work [10] proved the combination of both technologies, in the so-called CWPO-Photoassisted process, decreases the induction period, because of the role of UV in the Fe(II)/Fe(III) cycle. Despite this, the catalytic activity of ilmenite was lower when compared to other heterogeneous catalysts [11,12]. In this work, Temperature Programmed Reduction (TPR) is proposed to vary the Fe(II)/Fe(III) ratio on ilmenite surface, increasing the percentage of reduced iron species, which could enhance its catalytic activity.

In addition, light source is the other key point on CWPO-Photoassisted processes. In this sense, Light Emitting Diodes (LEDs) represent a reliable and feasible choice to replace conventional light sources in many applications. The main advantages include high photon efficiency, low voltage electrical power source, power stability, emission in broader spectral wavelength, and no need for cooling during long time operation for complete photocatalytic reactions [13,14].

Therefore, the aim of this work is to study the influence of reduction treatment (in H_2 atmosphere) on the physical and chemical properties of ilmenite as well as on their catalytic activity and stability for CWPO-Photoassisted process under LED light (405 nm).

2. Materials and methods

2.1. Catalysts physico-chemical characterization

The textural properties of the catalysts were determined by means of nitrogen adsorption–desorption isotherms at −196 °C using a Micromeritics Tristar 3020 apparatus. The samples were previously outgassed overnight at 150 °C to a residual pressure of 10^{-3} Torr.

The Ilmenite composition was obtained by total reflection X-ray fluorescence (TXRF), using a TXRF spectrometer 8030c. The crystalline phases were analyzed by X-ray diffraction (XRD) with a diffractometer (Siemens model D-5000) with Cu Kα radiation. To determine the oxidation state of Fe and Ti, the solids were also characterized by X-ray Photoelectron Spectroscopy (XPS) using a K-Alpha – Thermo Scientific equipped with a AlKa X-ray excitation source, (1486.68 eV). XPS data was fitted by XPSPeak 4.1.

2.2. CWPO-Photoassisted runs

CWPO-Photoassisted runs were performed in a counter-flow quartz concentric tubular reactor (100 mL useful volume). The aqueous solution (phenol and H_2O_2) and the catalyst coursed through the intermediate wall. Both were continuously recirculated (with a peristaltic pump) to maintain the catalyst suspended. A commercial LED strip (SMD 5050) was placed around the external wall of the reactor. The irradiance corresponding to LED radiation was 10 $W \cdot m^{-2}$. LED light emits at 405 nm with a power of 48 W.

All the experiments were carried out at 50 °C, an initial pH of 3 with 100 mg/L of aqueous phenol solution, 500 mg/L of H_2O_2 (that correspond to the stoichiometric amount needed for complete mineralization of phenol) and 450 $mg \cdot L^{-1}$ of catalyst.

2.3. Analytical methods

Phenol and aromatic oxidation by-products were measured by HPLC (Varian Pro-Star 240) using a diode array detector (330 PDA). A Microsorb C18 5 μm column (MV 100, 15 cm long, 4.6 mm diameter) was used as stationary phase and 1 $mL \cdot min^{-1}$ of 4 mM aqueous sulfuric solution was used as mobile phase. Short-chain organic acids were analyzed by an ion chromatograph (Metrohm 790 IC) using a conductivity detector. A Metrosep A supp 5–250 column (25 cm length, 4 mm diameter) was employed as stationary phase, while an aqueous solution containing 3.2 mM Na_2CO_3 and 1 mM $NaHCO_3$ was employed as mobile phase at a flowrate of 0.7 $mL \cdot min^{-1}$. Total organic carbon (TOC) was determined using a TOC analyzer (Shimadzu, model 5000A) and hydrogen peroxide concentration was measured by colorimetric titration using the $TiOSO_4$ method [15]. Leached iron was quantified by ortho-phenanthroline method [16].

3. Results

3.1. Ilmenite modification

Fig. 1 shows the Temperature Programmed Reduction (TPR) profile of the raw ilmenite under H_2 atmosphere in the range 25–1000 °C. As can be observed, TPR showed two reduction peaks, indicating two changes in the iron oxidation state. The first peak (around 500 °C) corresponds to the partial reduction of Fe(III) to Fe(II) (reaction 1) and the second one (around 950 °C) is related with reduction of Fe(II) to Fe(0) (reaction 2). Therefore, the catalyst obtained after reduction of raw ilmenite at 500 °C and 950 °C are named reduced ilmenite and highly reduced ilmenite.

$$\mathrm{ILM-Fe(III)/Fe(II)} \xrightarrow{H_2} \mathrm{ILM-Fe(II)} \qquad (500\,^{\circ}\mathrm{C}) \tag{1}$$

$$\mathrm{ILM-Fe(II)} \xrightarrow{H_2} \mathrm{ILM-Fe(0)} \qquad (950\,^{\circ}\mathrm{C}) \tag{2}$$

3.2. Catalysts characterization

The mineral ilmenite ($FeTiO_3$) has a hexagonal structure with two-third of octahedrical position occupied by cations. Fe and Ti

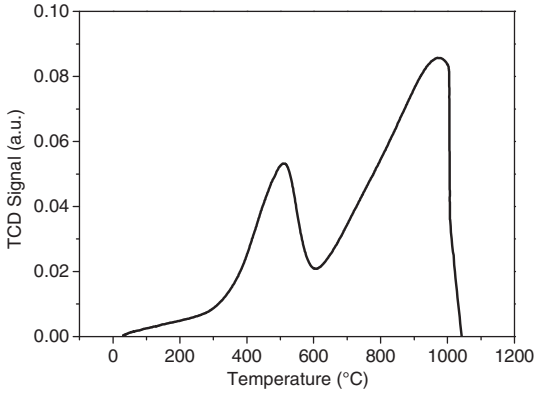

Fig. 1. TPR of raw ilmenite. Conditions: m = 0.05 g; Q_g = 40 $mL \cdot min^{-1}$, 5%H_2/Ar at 10 °C · min^{-1}.

are located in alternative layers. The weight percentage of Fe and Ti (Table S1) in this raw ilmenite was 36% and 37%, respectively (measured by TXRF). Ilmenite particles were mechanically milled down to dp < 100 μm measured with a 100 μm sieve. The textural analysis from N_2 adsorption–desorption isotherm (Fig. S1) indicates that ilmenite is a non-porous material with a BET Surface around 6 $m^2 \cdot g^{-1}$.

Fig. 2 shows the results of X-ray Diffraction (XRD) analysis of the three ilmenite catalysts. All diffraction lines obtained were compared to JCPDS card no. 21-1276 and 29-0733 due to TiO_2 Rutile phase and $FeTiO_3$ phase presence [17]. Intense peaks at $2\theta = 23.9°$, 32.65°, 35.3°, 40°, 48°, 53°, 61°, 63° indicating $FeTiO_3$ in the sample with a crystal size of 6.14 nm. Moreover the peaks at $2\theta = 27°$, 36°, 41°, 54° and 57° confirming rutile existence [17]. The three ilmenite materials are characterized by a mixed crystal phase composition. Raw and reduced ilmenites contained two phases: ilmenite phase (I) and rutile phase (R) in the relative intensity 85/15 and 70/30 respectively. In the case of highly reduced ilmenite, structural changes take place and new diffraction lines appear corresponding to metallic iron specie (Fe(0)) which correspond to the peaks $2\Theta = 45°$, 65° [18]. Highly reduced ilmenite contains a new crystalline phase and the relative intensity of them were 71/18/11 to metallic iron, rutile phase and ilmenite phase, respectively.

The catalysts were also characterized by XPS. Fig. 3 depicts the Fe 2p core level XPS spectra for the three catalysts. The XPS spectrum of the raw ilmenite catalyst shows two bands centered at binding energy values around 711.19 and 725.1 eV for Fe $2p^{3/2}$ and Fe $2p^{1/2}$, respectively, which can be attributed to Fe(III) [19,20]. On the other hand, the XPS spectrum of the reduced ilmenite catalyst shows that those bands are slightly displaced at binding energy values around 710.5 and 724.1 eV for Fe $2p^{3/2}$ and Fe $2p^{1/2}$, respectively, corresponding to Fe(II) [20]. A satellite band at 719 eV corresponding to Fe(III) can be observed in the case of the raw ilmenite catalyst. The presence of metallic iron was not clearly distinguishable in the XPS spectrum of the highly reduced catalyst since the two bands were not displaced to binding energies of 706.7 and 719.8, which are the specific ones for metallic iron [21]. This fact can be directly attributed to the low concentration of metallic iron present on the surface catalyst.

The fitted peaks in Fig. 3 indicate the surface amounts of Fe(II) and Fe(III). The calculated ratios Fe(II)/Fe(III) were 40/60, 60/40 and 62/38 for raw, reduced and highly reduced ilmenite, respectively [9]. Therefore, the reduction treatment increases the appearance of Fe(II) on the surface catalysts.

Fig. 4 shows the high-resolution Ti 2p spectral region of the ilmenite catalysts. The binding energy of the Ti $2p^{1/2}$ and Ti $2p^{3/2}$ core levels at 464.7 eV and 459.0 eV, respectively, together with their separation of 5.7 eV confirm the valence state of Ti as Ti(IV) in TiO_2 phase. XPS clearly suggests that there is no detectable Ti at lower oxidation state in the surface region of all samples, as indicated by the absence of the shoulder peaks associated with Ti(III) at

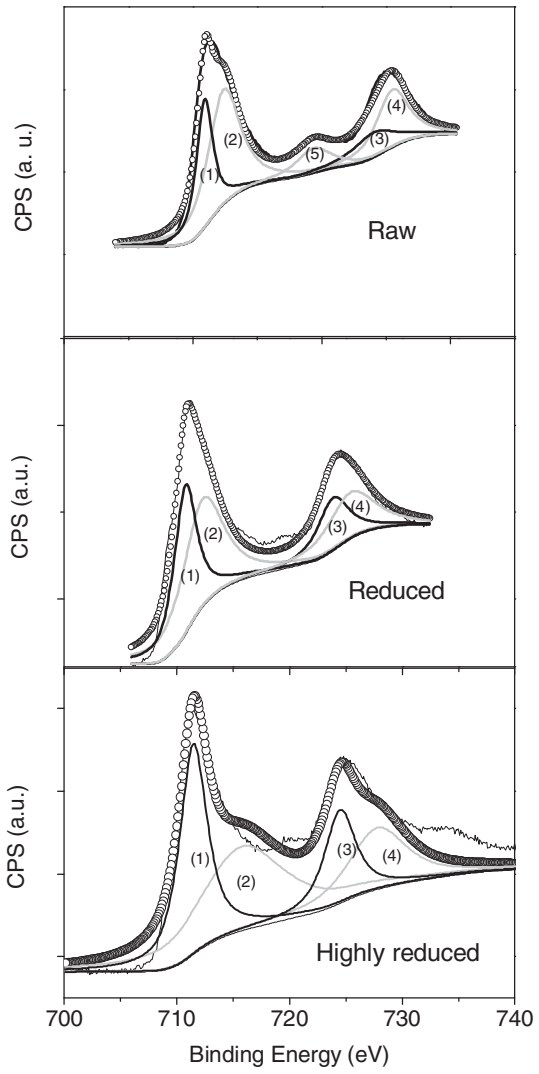

Fig. 3. Deconvolution of the Fe 2p core level for the ilmenite, reduced ilmenite and highly reduced ilmenite.

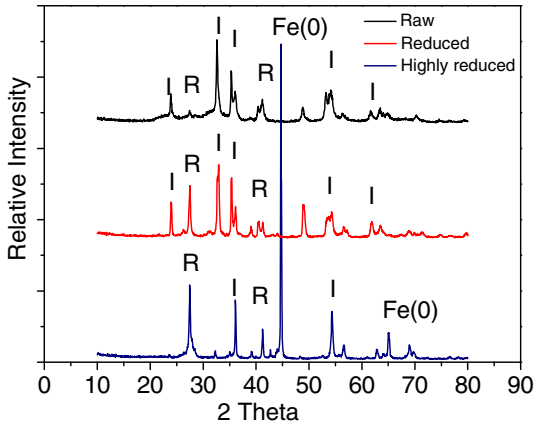

Fig. 2. XRD of the three catalyst: ilmenite phase (I), rutile phase (R) and metallic iron phase (Fe(0)).

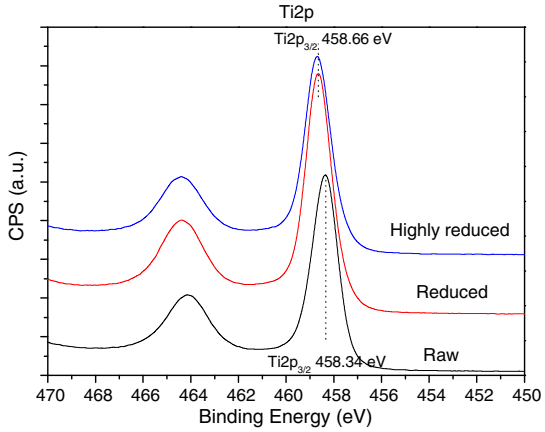

Fig. 4. XPS spectra of the Ti 2p core level for the three catalysts.

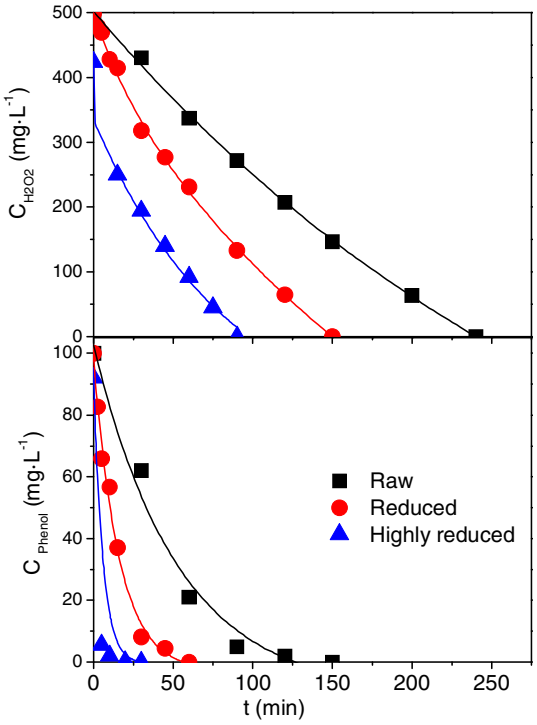

Fig. 5. H_2O_2 (a) and Phenol (b) concentration evolution for the three catalyst; Operating conditions: [cat] = 450 mg · L^{-1}, [H_2O_2] = 500 mg · L^{-1}, [Phenol] = 100 mg · L^{-1}, I = 10 W · m^{-2}. Lines show fitted data.

456.8 eV and 462.5 eV for $2p_{3/2}$ and $2p_{1/2}$ core level of Ti(III), respectively [22]. Raw ilmenite has a higher electronic density maybe due to lesser surface bonds with oxygen and surface groups.

3.3. CWPO-Photoassisted runs

The three solids were tested as catalysts in CWPO-Photoassisted process (Fig. 5). Raw ilmenite, reduced ilmenite and highly reduced ilmenite were able to decompose totally H_2O_2 within 240 min (Fig. 5a). However, the higher reduction degree, the higher decomposition rate, as show the H_2O_2 profiles.

This is related with the presence of different iron species [23] (reactions 3 and 4).

$$\text{ILM} - \text{Fe(II)} + H_2O_2 \rightarrow \text{ILM} - \text{Fe(III)} + HO^{\cdot} + OH^{-} \quad (3)$$

$$\text{ILM} - \text{Fe(III)} + H_2O_2 \rightarrow \text{ILM} - \text{Fe(II)} + H^{+} + HOO^{\cdot} \quad (4)$$

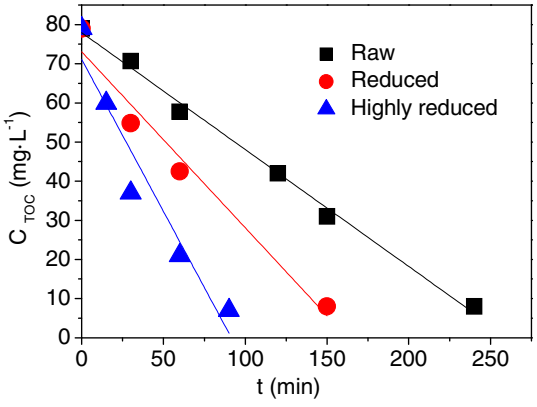

Fig. 6. TOC evolution for the three catalyst. Line shows linear fits. Table shows apparent kinetic constant rates. Operating conditions: [cat] = 450 mg · L^{-1}, [H_2O_2] = 500 mg · L^{-1}, [Phenol] = 100 mg · L^{-1}, I = 10 W · m^{-2}; λ = 405 nm. Lines show fitted data.

Table 1
Pseudo kinetic constant rate of H_2O_2, phenol and TOC for the three catalysts.

Catalyst	$k_{H_2O_2}$ (min^{-1})/R^2	k_{Phenol} (min^{-1})/R^2	$k_{TOC} \times 10^{-6}$ (M · s^{-1})/ R^2
Raw	0.0045/0.99	0.011/0.99	0.39/0.99
Reduced	0.0069/0.99	0.039/0.98	0.62/0.99
Highly reduced	0.0120/0.99	0.284/0.97	1.40/0.99

Table 2
Leached iron in solution after CWPO-Photoassisted runs.

Catalyst	Leached iron (mg · L^{-1})
Raw	<1
Reduced	2.6
Highly reduced	5.2

A similar trend was observed in the case of the phenol evolution (Fig. 5b), which indicates that H_2O_2 decomposition occurs mainly via HO· radicals. This is endorsed by the presence of hydroxylation by-products (catechol, hydroquinone and p-benzoquinone) in the reaction media during the early oxidation stages (Fig. S2) and traces of acetic, malonic and oxalic acids at the end of the reaction, once H_2O_2 was totally converted. It must be underlined that TOC reduction was close to 95% in all cases (Fig. 6). Therefore, the secondary H_2O_2 decomposition into H_2O and O_2 could be dismissed.

The evolution of phenol and H_2O_2 were fitted to a pseudo first-order model. The rate constants of raw, reduced and highly reduced ilmenite were 0.0045 min^{-1}, 0.0069 min^{-1} and 0.0120 min^{-1}, respectively for H_2O_2 and 0.011, 0.039 and 0.284 min^{-1}, respectively for phenol. On the other hand, a zero order kinetic was found to describe TOC evolution (Fig. 6) as usually occurs in photo-oxidation processes (Table 1). Nevertheless, as before, the TOC depletion rate became faster as the reduction degree increased. These results clearly confirm a straight relationship between the reduction treatment and the HO· production rate, that seems to be linked with the presence of reduced iron, Fe(II) and Fe(0), on the catalyst surface.

In a previous work [10] we demonstrated that the reduction of Fe(III) to Fe(II) by means of a solar light source (reaction 5) in

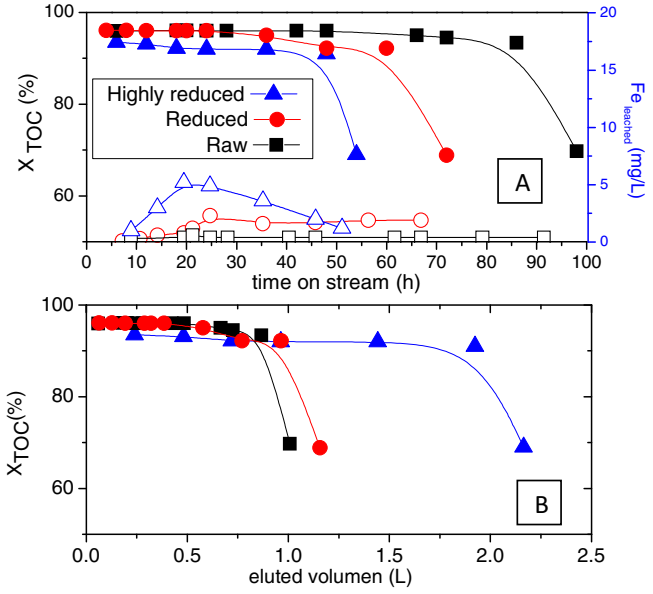

Fig. 7. Long-term experiments of the three catalysts. Operating conditions: [cat] = 450 mg · L^{-1}, [H_2O_2] = 500 mg · L^{-1}, [Phenol] = 100 mg · L^{-1}, I = 10 W · m^{-2}.

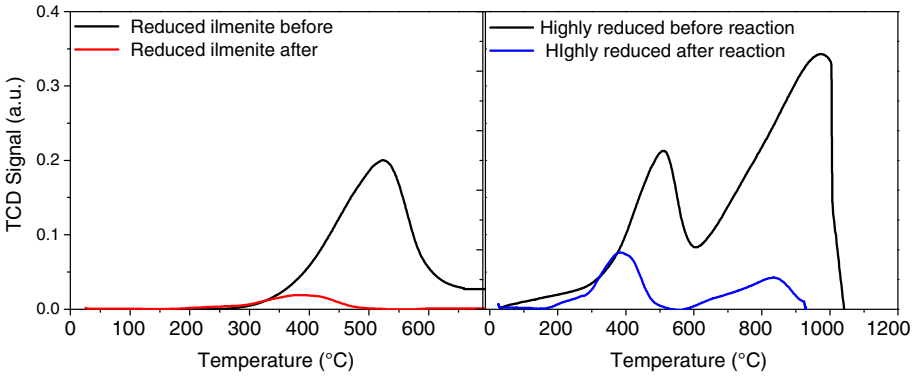

Fig. 8. TPR of catalysts after use. Reduced ilmenite in the left side and highly reduced ilmenite in the right side.

CWPO-Photoassisted treatments diminished the observed lag time when using raw ilmenite as catalyst.

$$\mathrm{ILM-Fe(III)} \xrightarrow{h\nu} \mathrm{ILM-Fe(II)} \quad (5)$$

Besides, reactions 6–8 explains the role of Fe(0) on this process [24]. The Fe(0) on the highly reduced ilmenite surface generates ferrous species (reaction 6) that reacts with H_2O_2, giving rise HO· and Fe(III) (reaction 7). Finally, Fe(0) is able to reduce Fe(III) to Fe(II) (reaction 8). This closed loop continues as long as H_2O_2 remains in solution [24]. This effect with iron reduction by the effect of light (reaction 5 and 9) causes a synergistic effect in oxidation reactions rates [25].

$$\mathrm{ILM-Fe(0)} \xrightarrow{H^+} \mathrm{ILM-Fe(II)} \quad (6)$$

$$\mathrm{ILM-Fe(II)} + H_2O_2 \rightarrow \mathrm{ILM-Fe(III)} + HO^{\cdot} \quad (7)$$

$$\mathrm{ILM-Fe(0)} + \mathrm{ILM-Fe(III)} \rightarrow \mathrm{ILM-Fe(II)} \quad (8)$$

$$\mathrm{ILM-Fe(II)} \xrightarrow{2e^-_{CB}} \mathrm{ILM-Fe(0)} \quad (9)$$

Fe(II) can be also reduced to Fe(0), when two electrons are captured from conduction band of titanium (reaction 10) [26].

$$\mathrm{ILM-Fe(II)} + 2\mathrm{ILM-Ti(III)} \rightarrow \mathrm{ILM-Fe(0)} + 2\mathrm{ILM-Ti(IV)} \quad (10)$$

The fact that iron is inside the crystal structure of the raw ilmenite, confers a significant stability to this catalyst, compared with supported iron catalysts [10]. Nevertheless, reduction treatments could modify this structure, affecting to the stability. Table 2 gathers the values of Fe leached for each catalyst at the end of the experiments.

As can be observed, the reduction treatment has a significant influence upon the catalyst stability, increasing the leaching of iron with the reduction temperature. However, in the worst scenario, the percentage of leached iron was less than 3% of the total iron contained in the catalyst, which is less than usually occurs with iron-supported catalysts [12]. It must be noted that the homogeneous Fenton contribution could be considered negligible due to the low H_2O_2 concentration remaining in the reaction media.

Unlike what occurs with other catalysts [27] there was no relation between the iron leached and the concentration of oxalic acid in the reaction medium (Fig. S3). It must be noted that in presence of iron based catalyst and UV below 500 nm, oxalic acid is easily decomposed, significantly reducing the leaching of iron and enlarging the life cycle of those catalysts [28].

To learn more on the catalyst stability, long-term experiments were performed at similar conditions as in the previous batch runs. An aqueous solution containing 100 mg · L^{-1} of phenol and 500 mg · L^{-1} H_2O_2 was continuously fed into the reactor, whereas the catalyst (450 mg · L^{-1}) remained in the reactor (by placing a line-filter in the outlet). Hydraulic residence times (HRT) of 0.42, 0.67 and 1.67 mL · min^{-1} were used for raw, reduced and highly reduced ilmenite, respectively.

As can be seen in Fig. 7a, the three catalysts showed a significant initial stability since TOC conversions (around 100%) were maintained within the first 50 h on stream. Beyond this time on stream, the catalysts suffered a steep deactivation. Nevertheless, since HRTs were not the same for each catalyst, those data could not be directly used to compare the influence of the reduction treatment upon the long-term catalyst stability. For that reason, we graphed TOC conversion *vs* eluted volume (Fig. 7b). As can be observed the highly reduced ilmenite showed the highest lifetime, maintaining the catalytic activity after almost an eluted volume three times higher than in the case of raw ilmenite.

In order to explain the steep deactivation, the exhausted catalysts were analysed by TPR. Data corresponding to raw, reduced and highly reduced ilmenite are shown in Fig. 8. The results confirm changes in the iron oxidation state on the surface after long-term continuous experiments. Certain amounts of iron have been oxidised to iron(II) and iron(III) after being employed in the process. However, the coexistence of the three iron species are the reason of the good activity and reactivity of these catalysts. Such coexistence was kept after 100 h on stream.

4. Conclusions

The reduction of the iron oxidation state on the ilmenite surface appears a feasible alternative to improve its catalytic activity and lifetime in CWPO-Photoassisted processes under LED light (405 nm). The amount of Fe(II) and Fe(0) on the surface increased with the reduction degree, as well as the H_2O_2 decomposition rate into HO· radicals. This led to a higher oxidation rate. A complete phenol degradation and 95% of TOC conversion were reached in batch runs with the stoichiometric dose of H_2O_2 and 450 mg · L^{-1} of catalyst at pH of 3 and 50 °C. However, the leaching of the active phase increased with the reduction degree, up to around 3% of the total iron amount in the catalyst. Despite this, long-term continuous experiments confirmed the feasibility of the reduction treatment to improve the catalytic activity and the lifetime of raw ilmenite. A steep deactivation that was observed in all cases was related to a progressive oxidation of the iron on the surface.

Acknowledgments

The authors wish to thank the Spanish MINECO for the financial support through the project CTQ2013-41963-R. The Comunidad Autónoma de Madrid is also gratefully acknowledge for the

financial support through the project S2013/MAE-2716. P. García-Muñoz acknowledges the UAM (Universidad Autónoma de Madrid) for his FPI-UAM 2013 pre-doctoral grant.

Appendix A. Supplementary data

Supplementary data associated with this article can be found, in the online version, at http://dx.doi.org/10.1016/j.cej.2016.05.093.

References

[1] EU Water Framework Directive (<http://ec.europa.eu/environment/water/water-framework/index_en.html>) (last access: 02/19/2016).
[2] C.E. Diaz-Uribe, W.A. Vallejo L, J. Miranda, Photo-Fenton oxidation of phenol with Fe(III)-tetra-4-carboxyphenylporphyrin/SiO_2 assisted with visible light, in: J. Photochem. Photobiol. A 294 (2014) 75–80.
[3] M. Minella, G. Marchetti, E. De Laurentiis, M. Malandrino, V. Maurino, C. Minero, Photo-Fenton oxidation of phenol with magnetite as iron source, in: Appl. Catal., B: Environ. 154–155 (2014) 102–109.
[4] E. Moctezuma, B. Zermeño, E. Zarazua, L. Torres-Martínez, R. García, Photocatalytic degradation of phenol with Fe-titania catalysts, Top. Catal. 54 (2011) 496–503.
[5] J.A. Zazo, J.A. Casas, A.F. Mohedano, J.J. Rodriguez, Semicontinuous Fenton oxidation of phenol in aqueous solution. A kinetic study, Water Res. 43 (2009) 4063–4069.
[6] J.A. Zazo, J.A. Casas, A.F. Mohedano, M.A. Gilarranz, J.J. Rodríguez, Chemical pathway and kinetics of phenol oxidation by Fenton's reagent, Environ. Sci. Technol. 39 (2005) 9295–9302.
[7] A. Teel, D. Finn, J. Schmidt, L. Cutler, R. Watts, Rates of trace mineral-catalyzed decomposition of hydrogen peroxide, J. Environ. Eng. 133 (2007) 853–858.
[8] Y.H. Chen, Synthesis, characterization and dye adsorption of ilmenite nanoparticles, J. Non-Cryst. Solids 357 (2011) 136–139.
[9] Y.R. Smith, K. Joseph Antony Raj, V. Subramanian, B. Viswanathan, Sulfated Fe_2O_3–TiO_2 synthesized from ilmenite ore: a visible light active photocatalyst, Colloids Surf. 367 (2010) 140–147.
[10] P. García-Muñoz, G. Pliego, J.A. Zazo, A. Bahamonde, J.A. Casas, Ilmenite ($FeTiO_3$) as low cost catalyst for advanced oxidation processes, J. Environ. Chem. Eng. 3–4 (2016) 542–548.
[11] J.A. Zazo, J. Bedia, C.M. Fierro, G. Pliego, J.A. Casas, J.J. Rodriguez, Highly stable Fe on activated carbon catalysts for CWPO upon $FeCl_3$ activation of lignin from black liquors, Catal. Today 187 (2012) 115–121.
[12] M. Munoz, Z. de Pedro, N. Menendez, J.A. Casas, J.J. Rodriguez, A ferromagnetic γ-alumina-supported iron catalyst for CWPO. Application to chlorophenols, in: Appl. Catal., B: Environ. 136-137 (2013) 218–224.
[13] W. Jo, R.J. Tayade, New generation energy-efficient light source for photocatalysis: LEDs for environmental applications, Ind. Eng. Chem. Res. 53 (2014) 2073–2084.
[14] M.R. Eskandarian, M. Fazli, M.H. Rasoulifard, H. Choi, Decomposition of organic chemicals by zeolite-TiO_2 nanocomposite supported onto low density polyethylene film under UV-LED powered by solar radiation, Appl. Catal. B: Environ. 4 (2016) 407–416.
[15] G. Eisenberg, Colorimetric determination of hydrogen peroxide, Ind. Eng. Chem. Anal. Ed. 15 (1943) 327.
[16] E.B. Sandell, Colorimetric determination of traces of metals, J. Phys. Chem. 49 (1945) 263–264.
[17] A.A. Baba, S. Swaroopa, F.A.Adekola. Ghoshmk, Mineralogical characterization and leaching behavior of Nigerian ilmenite ore, Trans. Nonferrous Met. Soc. China 23 (2013) 2743–2750.
[18] C. Huang, W. Hsieh, J.R. Pan, S. Chang, Characteristic of an innovative TiO_2/Fe^0 composite for treatment of azo dye, Sep. Pur. Tech. 58 (2007) 152–158.
[19] P. Mills, J. Sullivan, A study of the core level electrons in iron and its three oxides by means of X-ray photoelectron spectroscopy, J. Phys. D-Appl. Phys. 5 (1983) 723–732.
[20] T. Yamashita, P. Hayes, Analysis of XPS spectra of Fe^{2+} and Fe^{3+} ions in oxide materials, Appl. Surf. Sci. 2 (2008) 2441–2449.
[21] M. Descostes, F. Mercier, N. Thromat, C. Beaucaire, M. Gautier-Soyer, Use of XPS in the determination of chemical environment and oxidation state of iron and sulfur samples: constitution of a data basis in binding energies for Fe and S reference compounds and applications to the evidence of surface species of an oxidized pyrite in a carbonate medium, Appl. Surf. Sci. 4 (2000) 288–302.
[22] X. Xin, T. Xu, J. Yin, L. Wang, C. Wang, Management on the location and concentration of Ti^{3+} in anatase TiO_2 for defects-induced visible-light photocatalysis, Appl. Catal. B: Environ. 10 (2015) 354–362.
[23] R. Chen, J. Pignatello, Role of quinone intermediates as electron shuttles in Fenton and photoassisted Fenton oxidations of aromatic compounds, Environ. Sci. Technol. 31 (1997) 2399–2406.
[24] Y. Segura, F. Martínez, J.A. Melero, J.L.G. Fierro, Zero valent iron (ZVI) mediated Fenton degradation of industrial wastewater: treatment performance and characterization of final composites, Chem. Eng. J. 6 (2015) 298–305.
[25] S.C. Xu, S.S. Pan, Y. Xu, Y.Y. Luo, Y.X. Zhang, G.H. Li, Efficient removal of Cr(VI) from wastewater under sunlight by Fe(II)-doped TiO_2 spherical shell, J. Hazard. Mater. 2 (2015) 7–13.
[26] W. Hsieh, J.R. Pan, C. Huang, Y. Su, Y. Juang, Enhance the photocatalytic activity for the degradation of organic contaminants in water by incorporating TiO_2 with zero-valent iron, Sci. Total Environ. 1 (2010) 672–679.
[27] J.A. Zazo, J.A. Casas, A.F. Mohedano, J.J. Rodríguez, Catalytic wet peroxide oxidation of phenol with a Fe/activated carbon catalyst, Appl. Catal. B: Environ. 65 (2006) 261–268.
[28] J.A. Zazo, G. Pliego, P. García-Muñoz, J.A. Casas, J.J. Rodríguez, UV-LED assisted catalytic wet peroxide oxidation with a Fe(II)-Fe(III)/activated carbon catalyst, Appl. Catal. B: Environ. 192 (2016) 350–356.